environmental microbiology

Environmental Microbiology (2022) **24**(3), 1166–1182 doi:10.1111/1462-2920.15718

Microbial bioindicators of Stony Coral Tissue Loss Disease identified in corals and overlying waters using a rapid field-based sequencing approach

Cynthia C. Becker[1,2] **Marilyn Brandt**,[3] **Carolyn A. Miller**[1] **and Amy Apprill**[1*]

[1]*Marine Chemistry & Geochemistry, Woods Hole Oceanographic Institution, Woods Hole, MA.*

[2]*MIT-WHOI Joint Program in Oceanography/Applied Ocean Science and Engineering, Earth, Atmospheric and Planetary Sciences, Cambridge and Woods Hole, MA.*

[3]*University of the Virgin Islands, St. Thomas, USVI.*

Summary

Stony Coral Tissue Loss Disease (SCTLD) is a devastating disease. Since 2014, it has spread along the entire Florida Reef Tract and into the greater Caribbean. It was first detected in the United States Virgin Islands in January 2019. To more quickly identify microbial bioindicators of disease, we developed a rapid pipeline for microbiome sequencing. Over a span of 10 days we collected, processed and sequenced coral and near-coral seawater microbiomes from diseased and apparently healthy *Colpophyllia natans*, *Montastraea cavernosa*, *Meandrina meandrites* and *Orbicella franksi*. Analysis of bacterial and archaeal 16S ribosomal RNA gene sequences revealed 25 bioindicator amplicon sequence variants (ASVs) enriched in diseased corals. These bioindicator ASVs were additionally recovered in near-coral seawater (<5 cm of coral surface), a potential reservoir for pathogens. Phylogenetic analysis of microbial bioindicators with sequences from the Coral Microbiome Database revealed that *Vibrio*, *Arcobacter*, Rhizobiaceae and Rhodobacteraceae sequences were related to disease-associated coral bacteria and lineages novel to corals. Additionally, four ASVs (*Algicola*, *Cohaesibacter*, *Thalassobius* and *Vibrio*) were matches to microbes previously associated with SCTLD that should be targets for future research. Overall, this work suggests that a rapid sequencing framework paired with specialized databases facilitates identification of microbial disease bioindicators.

Introduction

Stony Coral Tissue Loss Disease (SCTLD) is a rapidly progressing, persistent and widespread coral disease that affects at least 24 reef-building coral species in the Caribbean (Florida Keys National Marine Sanctuary, 2018). Since 2014, when it was first detected off Miami-Dade county, FL, it has devastated Floridian reefs, where loss in live coral has been as high as 60% (Precht *et al*., 2016; Walton *et al*., 2018). In the following years, the disease spread over the entire Florida Reef Tract and in 2018, the disease had appeared in disparate areas of the Caribbean (Kramer *et al*., 2021). The SCTLD outbreak is one of the longest and most widespread coral disease outbreaks ever to be recorded (Rosales *et al*., 2020). The extended duration, widespread occurrence and high species susceptibility associated with SCTLD make this an unprecedented and devastating coral disease.

When SCTLD first emerged on Floridian reefs, it initially impacted species including *Meandrina meandrites*, *Dichocoenia stokesii*, *Dendrogyra cylindrus* (an Endangered Species Act-listed coral) and the brain corals (i.e. *Colpophyllia natans*, *Pseudodiploria strigosa*). In ensuing months after the initial outbreak, other species began to show signs of SCTLD, including bouldering-type corals such as *Montastraea cavernosa* and *Orbicella* spp. (Florida Keys National Marine Sanctuary, 2018). Similar assemblages of affected species and disease ecology confirmed the emergence of SCTLD on reefs off of Flat Cay, an unoccupied island off of St. Thomas, U.S. Virgin Islands (USVI), in January 2019. Tissue loss on USVI corals progress at rates up to 35-fold higher than other common coral diseases and leads to complete mortality of over half of afflicted colonies (Meiling *et al*., 2020). Throughout 2019, and until the time of sampling in February 2020, the disease spread around the

Received 10 February, 2021; revised 10 August, 2021; accepted 10 August, 2021. *For correspondence. E-mail aapprill@whoi.edu; Tel. (+01) 508 289 2649; Fax (+01) 508 457 2164.

island of St. Thomas and east to the island of St. John (VI-CDAC, 2021).

The causative agent(s) responsible for SCTLD remain elusive, a common feature of the majority of coral diseases (Mera and Bourne, 2018; Vega Thurber *et al*., 2020). Further, the lack of correlation between SCTLD severity and ambient temperature or chlorophyll concentrations, suggests that a novel, yet highly contagious, pathogen may be responsible (Muller *et al*., 2020). Successful cessation of lesion progression following application of amoxycillin paste to afflicted colonies suggests that either the pathogen(s) are of bacterial origin or that bacteria play a role in disease progression and virulence as opportunistic microbes (Aeby *et al*., 2019; Neely *et al*., 2020). To detect disease bioindicators, 16S ribosomal RNA (rRNA) gene sequencing approaches that target bacteria and archaea were employed on field-collected coral samples from the Florida Reef Tract, where the disease originated (Meyer *et al*., 2019; Rosales *et al*., 2020). Meyer *et al*. (2019) found bacteria from five genera, including *Vibrio*, *Arcobacter*, *Algicola*, *Planktotalea* and one unclassified genus that were consistently enriched in the lesion tissue of three species (*M. cavernosa*, *Diploria labyrinthiformis* and *Dichocoenia stokesii*). In a separate study (Rosales *et al*., 2020), Rhodobacterales and Rhizobiales sequences were associated with lesions in *Stephanocoenia intersepta*, *D. labyrinthiformis*, *D. stokesii* and *M. meandrites*. It remains to be seen if these same microbial taxa are associated within SCTLD lesions across the greater Caribbean, especially in the geographically distant USVI, as well as in other coral species affected by the disease.

With such a widespread occurrence, it is important to understand the ways in which SCTLD is transmitted. It is hypothesized that transmission of this disease is through the water column, as evidenced by tank-based experiments (Aeby *et al*., 2019) and modelling of likely dead coral material and sediments within neutrally buoyant water parcels (Dobbelaere *et al*., 2020). Additionally, disease-associated microbial taxa were recovered in water and sediment of diseased-afflicted coral reefs, indicating that sediment may also play a role in transmission (Rosales *et al*., 2020). Disease-associated taxa or putative pathogens have yet to be examined in seawater directly surrounding diseased coral colonies using a targeted sampling method, such as syringe-based water sampling over corals (Weber *et al*., 2019).

The seawater directly overlying coral, here termed 'near-coral seawater', is an important reef environment. Compared to surrounding reef seawater, this environment is characterized by microbes with unique metabolisms and more virulent-like and surface-associated lifestyles (Weber *et al*., 2019). Also, this near-coral seawater environment is hypothesized to be a recruitment zone for both symbiotic microorganisms and potential pathogens (Weber *et al*., 2019). While coral physiology may influence the microbes living in this environment, water flow and surrounding currents also play a role (Silveira *et al*., 2017). Given existing evidence and hypotheses that the SCTLD pathogen or pathogens are water-borne (Aeby *et al*., 2019; Dobbelaere *et al*., 2020; Rosales *et al*., 2020), directly targeting the zone of potential pathogen recruitment is important for supporting these claims.

The rapid spread, persistence and virulence of SCTLD make it imperative to develop speedier response procedures for understanding this disease. While microbial community profiling cannot verify candidate pathogens, it is one step in the process of elucidating SCTLD causation through identification of microbial indicators that can be tested further for their role in disease aetiology. Additionally, these methods offer a breadth of information, but can fall short in processing time. Typical microbiome pipeline procedures involve weeks to months of sample processing, sequencing and data analysis. Combined with the requirement for specialized equipment, these procedures are often difficult to conduct in remote island reef locations. Field-based sequencing circumvents these challenges and offers additional benefits, such as working immediately with fresh samples and in the case of marine disease studies, the quickly processed data could even inform sampling strategies during the timeline of the project (Apprill, 2019). Recently, Illumina developed the iSeq 100 System, a portable sequencing platform. The platform uses sequencing by synthesis chemistry combined with complementary metal-oxide semiconductor (CMOS) technology and produces 8 million reads, with greater than 80% of reads passing a quality score of Q30 (99.9% base call accuracy) in each run (Illumina, 2020). Additionally, the CMOS technology allows the sequencing to occur all in a small, single-use cartridge, contributing to its ease of use in mobile (e.g. ship) laboratory settings. More portable sequencing technology and the increasing availability of portable thermocycler machines and centrifuges have made it possible to set up molecular laboratories in almost any environment with an electrical connection.

Here, we developed and applied a rapid coral microbiome sequencing pipeline designed to more quickly gather data on the effects of SCTLD currently affecting numerous nations and reefs across the Caribbean. By setting up small, portable molecular biology tools in a home rental, we successfully collected, processed and sequenced diseased and apparently healthy coral and near-coral seawater samples at two reefs in St. Thomas, USVI (Fig. 1). We were interested in answering the following questions regarding the implementation of this rapid pipeline to more broadly understand the aetiology

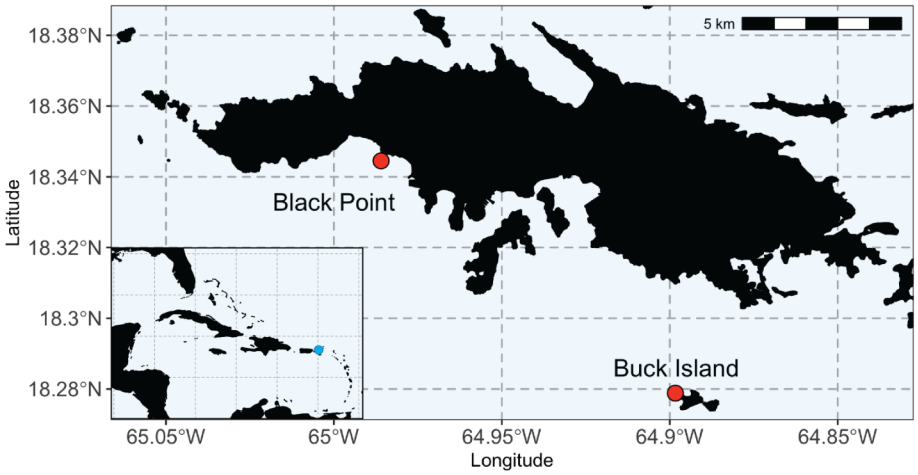

Fig 1. Sampling locations at Black Point and Buck Island reefs in St. Thomas, U.S. Virgin Islands. St. Thomas sampling locations included a reef at Black Point, which was experiencing SCTLD for 13 months prior to sampling and a reef at Buck Island, in which SCTLD broke out in the month prior. Scale bar is 5 km with marks at every kilometre. Inset map shows the greater Caribbean with the blue dot noting the location of the U.S. Virgin Islands.

of SCTLD: (i) How effective is a portable sequencing approach for coral disease studies and potentially other marine diseases, (ii) What microbial taxa are differentially distributed in healthy and diseased coral and which may be bioindicators of the disease, (iii) Can we identify SCTLD bioindicator microbes in the seawater directly overlying healthy and diseased corals and (iv) To what extent are these SCTLD bioindicators phylogenetically related to known or unknown coral-associated bacteria?

Results

Output of field-based sequencing in a portable microbiome laboratory

Three field-based sequencing runs with the Illumina iSeq 100 system each generated about 2 GB of paired-end, 150 bp sequencing data. In total, 12,997,634 sequencing reads were produced and used for subsequent data analysis. Each sequencing run lasted approximately 17 h and the runs were conducted on sequential days from February18th to 20th, 2020. The 3 days of sequencing produced high quality reads, with the forward reads containing 89.6%, 94.8% and 89.8% of reads having a Q30 score or better respectively. Following filtration of forward sequencing reads, the number of reads for the 49 coral samples ranged from 60,105 to 128,036, with an average of 99,177 (±14,511) while the range for the 51 seawater samples was 68,527 to 119,141, with an average of 96,933 (±10,218) (Supporting Information Table S2). Thus, all samples were successfully sequenced with sufficient sequence reads for downstream analysis (60,000+ sequences). The average numbers of sequences recovered from the controls were as follows (average ± 1SD, *n*): Syringe method control samples (96,290 ± 7542, $n = 9$), DNA extraction control samples (19,418 ± 11,672, $n = 6$) and PCR negative control samples (9930 ± 904, $n = 3$) (Supporting Information Table S2). Over the course of the three sequencing runs, the same mock community of 20 known bacteria was sequenced to verify consistency and success of sequencing and ASV generation over the three individual runs. Successful identification of all 20 exact amplicon sequence variants within the mock community was achieved from all three runs, though for each, additional sequence variants were also recovered (Fig. 2).

Health state determines coral microbiome structure while near-coral seawater microbiomes change according to site

Visualization of microbial beta diversity in corals using Principal Coordinates analysis (PCoA) of Bray–Curtis dissimilarity revealed significant changes in the coral microbiota associated with health condition, coral species and reef site (Fig. 3a, Supporting Information Figs. S1 and S2, Table 1). Permutational analysis of variance (PERMANOVA) tests comparing diseased ('DD'; $n = 21$) to healthy pooled from two sample types (healthy from diseased colonies, 'HD' and healthy from healthy colonies, 'HH'; pooling occurred because samples from apparently healthy colonies from all species was not available; $n = 28$) revealed disease state as having a significant effect on coral microbiome composition (Fig. 3a, $R^2 = 0.25$, $p < 0.001$). The effect of health state, irrespective of species, was slightly higher when split up by all three conditions ('HH', 'HD', 'DD', Fig. 3a, PERMANOVA, $R^2 = 0.26$, $p < 0.001$). The effect of species on structuring coral microbial communities was also significant, though the effect size was smaller than between healthy and diseased corals (Fig. 3a, Supporting Information Figs. S1–S3, PERMANOVA, $R^2 = 0.15$, $p < 0.001$). Interestingly, a PERMANOVA with disease state nested within coral species exerted an even greater effect,

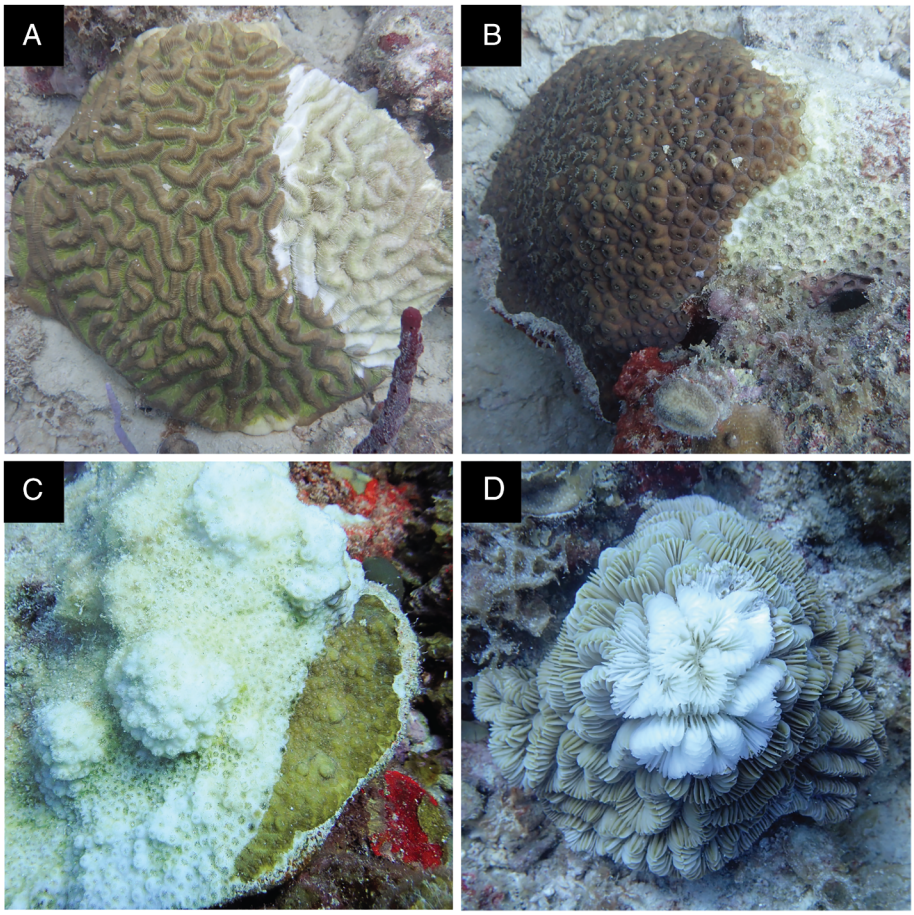

Fig 2. Stony Coral Tissue Loss Disease lesions progress across healthy tissue. Photos represent typical disease appearance on the following corals included in the present study: (a) *Colpophyllia natans*, (b) *Montastraea cavernosa*, (c) *Orbicella franksi*, (d) *Meandrina meandrites*. Seawater and coral were sampled at the lesion front and 10 cm away from the lesion, or as far as possible from the lesion, when possible.

explaining 36% of microbiome structure (Fig. 3a, $R^2 = 0.36$, $p < 0.001$). Together, disease state, species and the nested designation exerted a larger effect on the microbial community composition compared to site-based changes between Buck Island ($n = 30$) and Black Point ($n = 19$), though site did significantly structure the coral microbial communities (Fig. 3a, Supporting Information Figs. S2 and S3, Table 1, PERMANOVA, $R^2 = 0.041$, $p = 0.031$). Only two coral species, *C. natans* and *M. cavernosa*, were sampled at both Buck Island and Black Point. A PCoA of Bray–Curtis dissimilarity and subsequent PERMANOVA test on only those two species revealed site to be an insignificant factor in structuring the microbiome (Supporting Information Fig. S2, PERMANOVA, $R^2 = 0.04$, $p = 0.166$), compared to health state ('HH' and 'HD' vs. 'DD') (Supporting Information Fig. S2, PERMANOVA, $R^2 = 0.31$, $p < 0.001$).

Analysis of dispersion of beta diversity revealed significant differences between coral health states (healthy vs. diseased) (Fig. 3b). The distance to centroid of all healthy corals (HH and HD) was significantly lower, though more variable, than that of diseased corals (independent Mann–Whitney U Test, $p < 0.001$, Fig. 3b). Diseased microbiome beta diversity dispersion was higher and more consistent compared to healthy microbial beta diversity (Fig. 3b). Healthy coral microbiomes were generally less dispersed (more closely clustered in the PCoA) except for a few samples, which were dispersed farther from the other healthy samples (Fig. 3a,b). Furthermore, the range in raw Bray–Curtis dissimilarity values within each coral sample (healthy vs. diseased), reinforced the finding of increased beta diversity dispersion of diseased compared to healthy corals (Mann–Whitney *U* test $p < 0.001$; Supporting Information Fig. S4).

The effect of disease state was also visible in the stacked bar plot of coral microbiomes (Supporting Information Fig. S5). Notably, *M. cavernosa* contained increased relative abundances of Deltaproteobacteria in diseased corals (Supporting Information Fig. S5b). *Clostridia* and *Campylobacteria* relative abundances were increased in diseased corals, though *Clostridia* was most prominent in diseased *M. cavernosa* and *C. natans*, while *Campylobacteria* was most prominent in diseased *O. franksi* (Supporting Information Fig. S5). Interestingly, Oxyphotobacteria (predominantly *Prochlorococcus* and

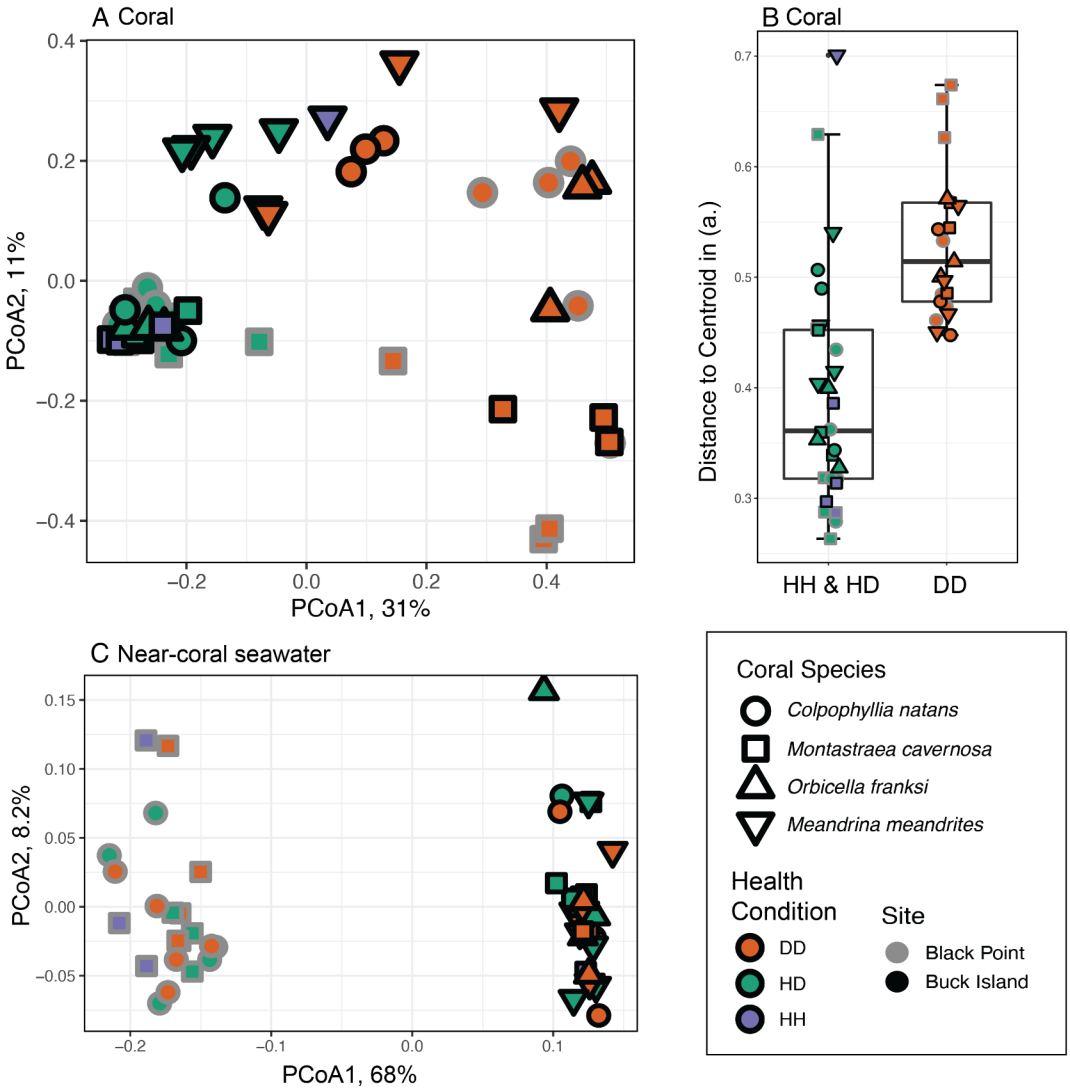

Fig 3. Coral microbiomes differed according to health condition and near-coral seawater microbiomes differed according to site. (a) Principal coordinate analysis (PCoA) displays Bray–Curtis dissimilarity of coral microbial communities, (b) beta diversity dispersion of coral microbiomes represented by boxplots of the distance to centroid in (a), and (c) PCoA of Bray–Curtis dissimilarity in near-coral seawater microbiomes. Fill colour represents health condition of the sample as diseased (DD, orange), healthy sample from a diseased colony (HD, green), or healthy sample from an apparently healthy colony (HH, purple). Outline colour indicates the reef where the sample was taken, which had either existing SCTLD infection (Black Point, grey), or was experiencing a recent (<1 month) outbreak of SCTLD (Buck Island, black). Shape represents species of coral sampled: *Colpophyllia natans* (circle), *Montastraea cavernosa* (square), *Orbicella franksi* (up triangle), and *Meandrina meandrites* (down triangle).

Table 1. Number of near-coral seawater (SW) and coral samples collected from Buck Island or Black Point reefs on St. Thomas, USVI.

	Buck Island			Black Point		
	HH	HD	DD	HH	HD	DD
Colpophyllia natans	0	3	3	0	5	5
Montastraea cavernosa	3	3	3	3 SW[a] 1 Coral[a]	4 SW[a] 5 Coral[a]	4 SW[a] 3 Coral[a]
Orbicella franksi	0	3	3	0	0	0
Meandrina meandrites	1	4	4	0	0	0

[a]Sample sizes from *M. cavernosa* from the Existing disease reef were different between seawater and coral due to sampling and processing constraints.

Synechococcus) decreased in relative abundance in diseased coral (Supporting Information Fig. S5).

Near-coral seawater microbiomes ($n = 51$, Table 1) taken within 5 cm of the coral surface were clearly distinct from coral microbiomes ($n = 49$, Table 1), but structured according to site (PERMANOVA $R^2 = 0.67$, $p < 0.001$) and not disease state (PERMANOVA $R^2 = 0.005$, $p = 0.921$) (Fig. 3c, Supporting Information Fig. S1). Coral species also significantly affected the composition of the overlying seawater (Fig. 3c, PERMANOVA, $R^2 = 0.22$, $p = 0.004$).

Coral disease bioindicators

To detect potential bioindicators of SCTLD, we used the beta-binomial regression model of the *corncob* R package (Martin *et al*., 2020) to test for differentially abundant ASVs between healthy (HH and HD) and diseased (DD) corals individually for each species (Table 1 for sample replication). The model recovered 25 ASVs that were significantly more abundant, that is, enriched and herein referred to as bioindicators, in the diseased sample of at least one of the coral species (Fig. 4, Supporting Information Table S3, Figs. S6–S9). Ten of those 25 ASVs were enriched in diseased samples of more than one coral species but none were enriched in all species (Supporting Information Table S3, Figs. S6–S9). Nonetheless, some ASVs, such as ASV44 (*Fusibacter*), were enriched in diseased coral from all species, though the trend was not always significant. The 25 bioindicator ASVs classified as belonging to 12 Families and 14 genera. Families with multiple bioindicator ASVs were Arcobacteraceae, Desulfovibrionaceae, Family XII of the order Clostridiales, Rhodobacteraceae and Vibrionaceae (Supporting Information Table S3). Within these, four ASVs belonged to the genera *Arcobacter*, five to *Vibrio* and three to *Fusibacter*.

In addition to identifying ASVs enriched in diseased coral, the differential abundance analysis revealed other ASVs that were depleted in diseased relative to healthy samples and were therefore healthy coral-associated (coefficient < 0, Supporting Information Figs. S6–S9). *M. meandrites* had only one ASV enriched in healthy samples (Family Terasakiellaceae from Rhodospirillales; Supporting Information Fig. S9). Healthy samples of *C. natans* (Supporting Information Fig. S6) and *M. cavernosa* (Supporting Information Fig. S7) were enriched with ASVs belonging to Clades Ia, Ib and unclassified Clade II of SAR11, the NS4 Marine Group and NS5 Marine Group of Flavobacteriaceae, *Prochlorococcus* MIT9313, *Synechococcus* CC9902 and unclassified SAR116. Healthy *C. natans* also was enriched in ASVs belonging to unclassified Rhodobacteraceae, Clade 1a Lachnospiraceae and OM60 (NOR5) clade of Halieaceae. Unique healthy-associated ASVs in *M. cavernosa* included 11 diverse taxa (Supporting Information Fig. S7). Healthy coral-associated ASVs from *O. franksi* largely represented taxa found in healthy corals from at least one of the other species targeted in this study (Supporting Information Fig. S8). One unclassified Arcobacteraceae ASV was associated with healthy *O. franksi*, as well as two *Endozoicomonas* ASVs (ASV99, ASV108).

Disease bioindicator taxa recovered within near-coral seawater

Previous studies indicated that seawater may be a vector for the SCTLD pathogen(s); therefore, we hypothesized that the seawater within 5 cm of coral lesions would harbour the 25 SCTLD bioindicator ASVs we identified from corals. A differential abundance test of the 25 bioindicator ASVs in seawater overlying disease lesions (DD, $n = 22$, Table 1) compared to healthy corals (HH and HD, $n = 29$, Table 1) did not find significant enrichment of those ASVs in seawater over diseased lesions. We further tested the 25 bioindicator ASVs in near-coral seawater over apparently healthy colonies compared to disease lesion colonies of *M. cavernosa*, the only species for which we had sufficient replication of apparently healthy colonies and found no ASV significantly enriched in waters overlying diseased corals. Despite the lack of significant enrichment of putative pathogens within near-coral lesion seawater, we did observe all 25 bioindicator ASVs in the near-coral seawater over diseased corals, except for two ASVs (*Cohaesibacter* ASV226 and *Desulfovibrio* ASV185). Several of the SCTLD-associated ASVs were present in seawater overlying all four diseased coral species, including *Algicola* (ASV52), *Arcobacter* (ASV21, ASV101), *Halodesulfovibrio* (ASV13), *Marinifilum* (ASV39) and *Vibrio* (ASV20) (Fig. 5). Interestingly, ASV34, an unclassified Rhodobacteraceae, was found only in near-coral seawater directly overlying disease lesions, but not over healthy corals across all species (Fig. 5). Overall, disease-enriched bacteria were identified at low levels (<1.5% relative abundance) in near-coral seawater, though there was no significant enrichment of these taxa over diseased coral.

Phylogenetic analysis of SCTLD-enriched taxa

Given the high representation of *Arcobacter*, *Vibrio*, Rhizobiaceae and Rhodobacteraceae ASVs in the bioindicator ASVs, we produced phylogenetic trees to better predict species-level identifications and to relate the ASVs to other sequences associated with coral disease, sequences from the Coral Microbiome Database

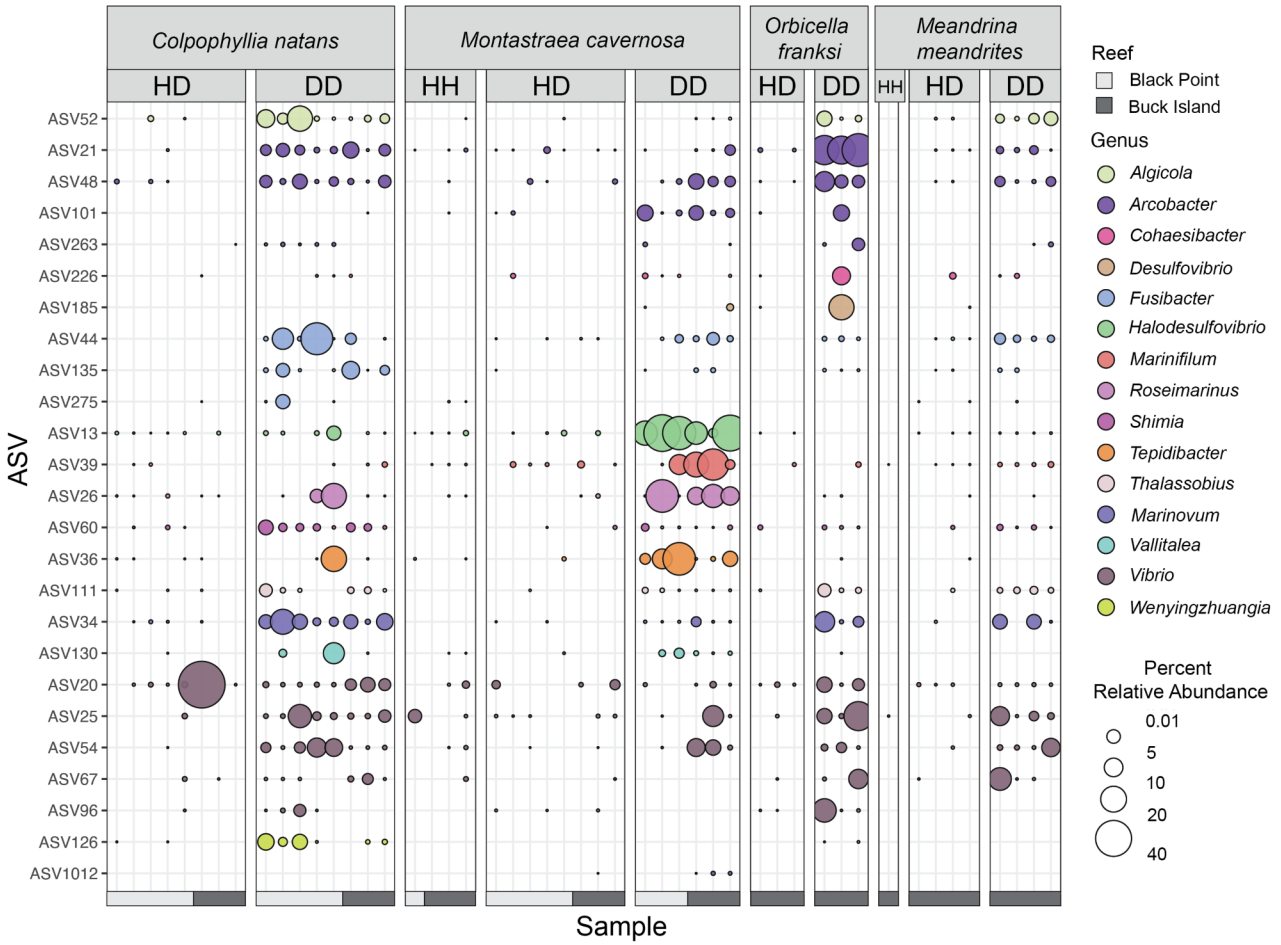

Fig 4. Relative abundances of 25 SCTLD bioindicator ASVs significantly differentially enriched (FDR corrected p-value < 0.05) in diseased coral of at least one coral species. Samples on the x-axis are organized by coral species (*Colpophyllia natans*, *Montastraea cavernosa*, *Meandrina meandrites*, and *Orbicella franksi*), health state of the coral (healthy sample from apparently healthy colony = 'HH', healthy sample from diseased colony = 'HD', disease lesion = 'DD'). Additionally, a colour bar at the bottom indicates the coral was collected at the Black Point (light grey) or at the Buck Island (dark grey). ASVs on the y-axis are organized and coloured by Genus. Percent relative abundance of each ASV is represented by the size of the coloured circle, with a percent relative abundance of zero represented by the absence of a circle or dot. The relative abundances were calculated after removing common seawater bacteria and archaea, which were determined using the syringe method control samples containing ambient reef seawater and with the R-package *decontam* (see methods).

(Huggett and Apprill, 2019) and SCTLD-associated ASV sequences reported from two previous studies (Meyer *et al*., 2019; Rosales *et al*., 2020). Phylogenetic analysis of the Campylobacterota (formerly Epsilonbacteraeota) genus *Arcobacter* spp. indicated no close relationship of the SCTLD-associated ASVs to described *Arcobacter* isolates. Instead, all SCTLD-associated ASVs grouped in clades with coral-associated or coral disease sequences (Supporting Information Fig. S10).

Phylogenetic analysis of the SCTLD bioindicator ASVs from the gammaproteobacterial genus *Vibrio* leveraged a reference tree previously constructed using existing coral-associated sequences found in the Coral Microbiome Database (Huggett and Apprill, 2019), *Vibrio* type strains and a SCTLD-associated *Vibrio* ASV by Meyer *et al*. (2019). ASV20 displayed high sequence identity to *V. harveyi* ATCC 35084, an isolate obtained from a brown shark kidney following a mortality event (formerly known as *Vibrio carchariae* (Grimes *et al*., 1984; Pedersen *et al*., 1998) (Supporting Information Fig. S11). Interestingly, *Vibrio* ASV54 in the present study was an exact sequence match to a longer (253 bp) SCTLD-associated ASV reported previously (Meyer *et al*., 2019) and this sequence is novel to corals (Table 2, Supporting Information Fig. S11). The remaining bioindicator ASVs 96, 67 and 25 all displayed high sequence identity to other coral-associated *Vibrio* sequences (Supporting Information Fig. S11).

We produced a phylogenetic tree with all known SCTLD-associated ASVs that classified to Rhizobiaceae,

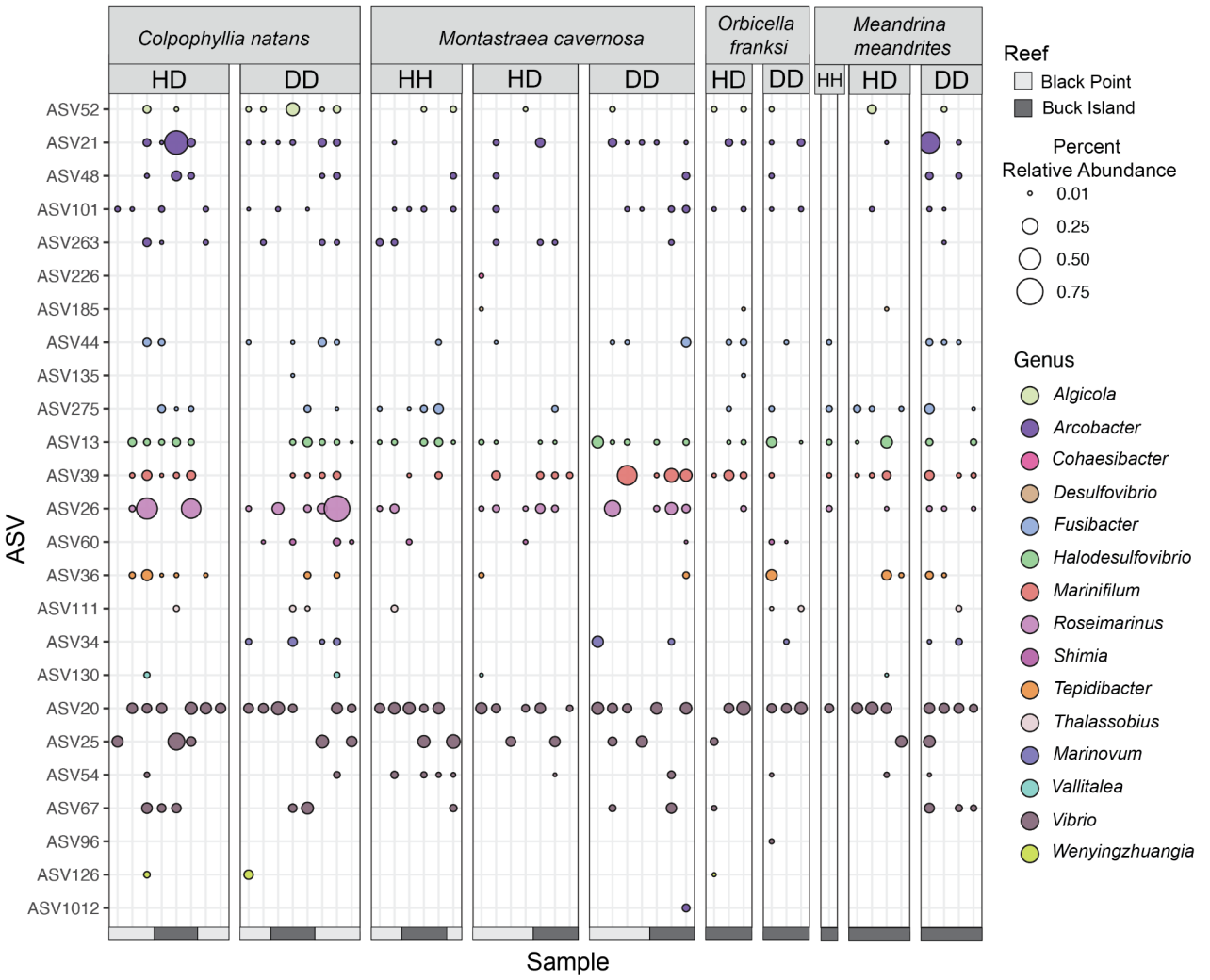

Fig 5. SCTLD bioindicator ASVs identified in coral were found in near-coral seawater. Samples on the *x*-axis are organized by coral species (*Colpophyllia natans*, *Montastraea cavernosa*, *Meandrina meandrites*, and *Orbicella franksi*), and health state of the coral (healthy sample from apparently healthy colony = 'HH', healthy sample from diseased colony = 'HD', disease lesion = 'DD'). Additionally, a colour bar at the bottom indicates whether the coral was collected at Black Point (light grey) or at Buck Island (dark grey). ASVs on the y-axis are organized and coloured by genus. Percent relative abundance of each ASV is represented by the size of the coloured circle, with a percent relative abundance of zero represented by the absence of a circle or dot. ASVs graphed are those identified by differential abundance analysis as significantly enriched in diseased coral (FDR corrected *p*-value <0.05) of at least one coral species.

Table 2. Bioindicator ASVs in the present study with 100% sequence similarity over 126 bp to SCTLD-associated ASVs of a longer length (~253 bp) identified by previous studies.

Family	Genus	ASV ID in present study	Enriched in diseased coral (Rosales *et al*. 2020)	Enriched in diseased coral (Meyer *et al*. 2019)
Pseudoalteromonadaceae	*Algicola*	52	No	Yes
Rhizobiaceae	*Cohaesibacter*	226	Yes	No
Rhodobacteraceae	*Thalassobius*	111	Yes	No
Vibrionaceae	*Vibrio*	54	No	Yes

sequences from other coral disease studies and other related sequences (Supporting Information Fig. S12). One bioindicator ASV from the present study (ASV226) was identical in the 126 bp overlapping region to a previous SCTLD-associated ASV11394 (Rosales *et al*., 2020) and both grouped with *Cohaesibacter marisflavi*, a bacterium that has been isolated from seawater (Table 2, Supporting Information Fig. S12). ASV18209

and ASV19474 also fell within the *Cohaesibacter* genus, close to sequences isolated from White Plague-affected corals (Supporting Information Fig. S12). SCTLD-associated ASV19959, ASV30828 and ASV16110 from Rosales *et al*. (2020) were most closely related to *Pseudovibrio denitrificans* NRBC 100300 (Supporting Information Fig. S12). Finally, the unclassified Rhizobiaceae ASV34211 and ASV24311 (Rosales *et al*., 2020) were closely associated to isolates of *Hoeflea* spp. and *Filomicrobium* spp., respectively (Supporting Information Fig. S12).

Phylogenetic analysis of SCTLD bioindicators that classified as Rhodobacteraceae using a reference tree generated from the Coral Microbiome Database (Huggett and Apprill, 2019) revealed close classification to bacteria associated with coral hosts that were distinct from existing isolates (Supporting Information Fig. S13). Several SCTLD-associated ASVs from Rosales *et al*. (2020) (ASV15252, ASV24736, ASV13497, ASV3538 and ASV29944) were related to sequences from ballast water and hypersaline mats rather than coral sequences (Supporting Information Fig. S13). In contrast, the SCTLD bioindicator ASV60 from the present study had high sequence identity to other coral-associated Rhodobacteraceae sequences with no definitive classification, though related to *Phaeobacter* (Supporting Information Fig. S13). Several Rhodobacteraceae ASVs classified to *Thalassococcus* sequences (ASV29894, ASV25482, ASV29283 from Rosales *et al*. (2020)) and ASV111 from the present study (exact sequence match to ASV29283 from Rosales *et al*. (2020)). Finally, SCTLD-associated ASV34 classified within the likely *Marinovum* genus alongside many coral-associated sequences (Supporting Information Fig. S13).

Discussion

To better understand the effect of Stony Coral Tissue Loss Disease on coral reefs in the U.S. Virgin Islands, an area with an active and detrimental SCTLD outbreak (VICDAC, 2021), we developed and integrated a rapid, field-based 16S rRNA gene sequencing approach to characterize microbiomes of coral and near-coral seawater of SCTLD-infected colonies. St. Thomas, USVI does not have a molecular ecology laboratory or sequencing facility; therefore, we transformed a home rental on the island to a molecular laboratory and in the span of 2 weeks, we carried out a complete microbiome workflow, from sample collection to sequencing. This short timeline enabled us to process fresh samples, gather data more quickly and begin data analysis in the following months, which revealed significant differences between healthy and diseased coral, regardless of coral species or reef location. Differential abundance analysis identified 25 SCTLD bioindicators, all of which were present in the seawater directly overlying coral. Furthermore, these bioindicator ASVs represented sequences with high sequence identity to the 16S sequence of the *Vibrio harveyi* pathogen, as well as sequences previously identified in diseased corals.

SCTLD lesion microbial communities are unique from healthy microbial communities

We identified clear and consistent differences between healthy and diseased coral microbiomes, regardless of location and species of coral. In addition, the dispersion of beta-diversity was consistently higher among the diseased corals, compared to all healthy corals, which had reduced, yet more variable dispersion of beta diversity. This greater beta diversity across diseased coral microbiomes could be indicative of some level of microbial dysbiosis associated with disease (MacKnight *et al*., 2021). Alternatively, the syringe-based collection method results in a homogenate of newly compromised, diseased tissue, as well as necrotic or sloughed off tissue that likely captures potential pathogen(s), organisms involved in secondary infections, or even saprophytic microorganisms proliferating off the exposed skeleton and dead coral tissue (Burge *et al*., 2013; Egan and Gardiner, 2016). For example, the finding of increased Deltaproteobacteria in diseased samples of *M. cavernosa* and the significant enrichment of *Halodesulfovibrio*, known sulfate-reducing bacteria, may have been a signature of the exposed coral skeleton (Chen *et al*., 2021), or perhaps anaerobic degradation of coral tissue (Viehman *et al*., 2006). Overall, the finding that disease impacts coral microbiome structure in the USVI is supported by previous findings that show shifts in coral microbiomes between healthy and diseased corals in Florida, USA (Meyer *et al*., 2019; Rosales *et al*., 2020).

While this study did not identify causative agents of SCTLD, the differential abundance analysis between healthy and diseased coral microbial communities revealed 25 disease bioindicator ASVs, which may represent potential pathogens or opportunistic bacteria relevant for future experimental work. Of these, we identified one ASV (ASV20), with 100% similarity in the overlapping region to *V. harveyi* (EU130475.1), a pathogen isolated from a shark mortality event and shown to be virulent for spiny dogfish (*Squalus acanthias*) (Grimes *et al*., 1984). This ASV was consistently detected in diseased coral (DD samples), including all *C. natans*, *M. meandrites* and *O. franksi* colonies and two-thirds of the *M. cavernosa* colonies, at relative sequence abundances of 5% or lower. Additionally, this ASV was frequently recovered in the HD and HH colonies, and most

near-coral seawater samples, indicating its broad prevalence in these diseased reefs. Interestingly, *V. harveyi* has been suggested as the causative agent of white syndrome disease in aquaria and field-based corals (Luna *et al*., 2010). Despite the prevalence of *V. harveyi* sequences in the present SCTLD study, this was not a SCTLD-associated bacterium identified in the Florida-based studies. Still, it seems relevant to examine pathogenicity of *V. harveyi* in future coral disease experiments.

Four of our SCTLD bioindicator ASVs were identical to ASVs identified in Florida-based SCTLD studies. *Algicola* ASV52 and *Vibrio* ASV54 were identical to ASVs identified in Florida by Meyer *et al*. (2019). These sequences have been associated with coral disease in the past (black band disease or white plague disease type II; reviewed by Meyer *et al*. 2019), but were phylogenetically distinct from other known coral-associated lineages (Supporting Information Fig. S11). Furthermore, although not significant in all coral species, the noticeable enrichment in abundance of both ASV52 (*Algicola*) and ASV54 (*Vibrio*) in corals may be biologically relevant, given their association with SCTLD-affected corals sampled in Florida approximately 1800 km away (Meyer *et al*., 2019).

Two other bioindicator ASVs in the present study, *Cohaesibacter* (ASV226) and *Thalassobius* (ASV111), matched identical regions of ASVs enriched in a study of Florida-based SCTLD-associated microbiomes by Rosales *et al*. (2020). In our study, *Cohaesibacter* ASV226 was enriched in diseased *O. franksi*, but barely detected in other corals. Rosales *et al*. (2020) detected the same ASV in Stephanocoenia *intercepta*, *D. labyrinthiformis*, and *M. meandrites* affected by SCTLD. Phylogenetic analysis placed those two similar sequences (ASV226 and ASV11394, Supporting Information Fig. S12) with *C. marisflavi*, a species not currently known to be a pathogen (Qu *et al*., 2011). Although no *Cohaesibacter* species are known pathogens, *C. intestini* was isolated from the intestine of an abalone (Liu *et al*., 2019). Two *Cohaesibacter* sequences identified by Rosales *et al*. (2020) were related to sequences previously isolated in cases of coral disease, indicating *Cohaesibacter* may be an important target for future study. Additionally, *Thalassobius* (ASV111) was an exact match to one of eight Rhodobacteraceae ASVs enriched in diseased corals in the Rosales *et al*. (2020) study. In the present study, this ASV was significantly enriched only in *C. natans*, but was generally present in all diseased corals. Furthermore, these ASVs, and two other disease-associated ASVs (ASV29894 and ASV25482) from Rosales *et al*. (2020) classified as unique unclassified coral bacteria and coral white plague disease afflicted respectively. Interestingly, several of the SCTLD-associated ASVs added into the Rhodobacteraceae phylogenetic tree were more closely associated to sequences from hypersaline mat or ballast water environments than coral-associated sequences. Despite variability in putative identity of the diverse Rhodobacteraceae sequences associated with SCTLD, exact sequences recovered from diseased corals across geographic regions in the Caribbean (Florida, USA, and USVI) may indicate some concordance in the effect of this disease on different coral species regardless of geography.

It should be noted that there are some methodological differences between the SCTLD studies, which could impact the microbial sequences recovered and compared. The studies all utilized the same primers, but the sequencing platforms differed in read length; the previous studies used merged reads, enabling a total read length of approximately 253 bp, whereas this study used 126 bp forward reads due to sequencing of primers. Although our amplicons are shorter and we only used forward reads, classification and taxonomic certainty does not decrease linearly with amplicon size, and may be between 71.1% and 83.2% accurate at the genus level compared to full length small subunit rRNA sequences (Wang *et al*., 2007) and even up to 99% confident at the phylum level compared to the approximately 253 bp V4 region targeted by the 515F and 806R primers (Liu *et al*., 2020). Despite this, it should be noted that identical 16S rRNA sequences do not always indicate identical species or genera, when analysed at the whole genome level (Stackebrandt and Goebel, 1994). All three studies compared here employed the DADA2 analysis pipeline, resulting in sequences published alongside ASV identifiers, allowing for comparison of amplicon sequence variants across studies, a significant benefit of the DADA2 pipeline (Callahan *et al*., 2017). Lastly, we did take care to insert the shorter amplicon sequences into a phylogenetic framework based on longer read sequences. Overall, the placement of the ASVs appear robust, but additional marker genes or genomes are necessary to confirm the taxonomies affiliated with the ASV-based sequences.

Similar to previous reports for white plague disease, it could be that both bacteria and viruses play a role in SCTLD onset and virulence. Antibiotic pastes containing amoxicillin have been shown to be effective at slowing and halting progression of SCTLD (Aeby *et al*., 2019; Neely *et al*., 2020). Despite this, we cannot rule out the role of viruses in this disease, which have been shown to play a role in white-plague-like diseases (Soffer *et al*., 2014). We did not investigate viruses in our study, but metagenomic and microscopic techniques that investigate holobiont components, such as bacteria, archaea, DNA and RNA-based viruses, and fungi, should be employed in the future. Finally, due to limited availability, this study lacks replication of samples from apparently healthy colonies ('HH') and future work could aim to

prioritize collection of samples from apparently healthy colonies, as it would serve as an important baseline for comparison.

Signals of SCTLD infection in near-coral seawater

Bioindicator microbes identified as SCTLD-enriched were broadly recoverable in near-coral seawater (<5 cm) surrounding the coral colonies, in agreement with a current hypothesis that seawater is the disease vector (Aeby *et al*., 2019). However, seven ASVs were found in fewer than five of the nine samples. According to the differential abundance comparison, none of the disease bioindicator ASVs were significantly enriched in seawater overlying diseased compared to healthy areas of the corals, though the relative closeness (<30 cm) between healthy and diseased seawater samples may have mixed this signal. The largest driver of differences in near-coral seawater microbial communities was location. The two reefs we sampled were distinct reefs approximately 12 km away from each other and featured overall similar environmental conditions (Supporting Information Table S1).

Beyond seawater, recent evidence suggests that sediments surrounding coral may play an important role as a reservoir of SCTLD pathogens (Rosales *et al*., 2020) though that was not sampled here. Future investigations into SCTLD vectors should aim to sample both near-coral sediments and seawater, both *in situ* and in isolated mesocosm tanks to provide further information on the likely modes of transmission of SCTLD pathogens.

Rapid and portable microbiome profiling is feasible and applicable to marine diseases

Here we successfully implemented an in-the-field microbiome protocol to rapidly gather data on microbiome composition associated with the destructive coral disease, SCTLD. Illumina launched the iSeq 100 System only recently, in 2018. It is the smallest (1 ft cube), cheapest, and most portable Illumina technology to date and features a single-use cartridge that houses all sequencing reagents, further contributing to its ease of use. Following three sequencing runs, the number of reads generated by the iSeq per sample was comparable to those recovered in a previous study of SCTLD microbiomes that used MiSeq sequencing for the same region of DNA and the same sample collection method (Meyer *et al*., 2019). Overall, the Illumina iSeq 100 System could be an ideal target for future studies on marine disease outbreaks, when there is a need for rapid information and results to better inform remediation and management of such disease outbreaks.

The present workflow could be applied again to SCTLD research, with some improvements. Although the data were gathered within 10 days of the project start, data analysis still took months. To circumvent this, all data analysis scripts are saved and easily accessible on GitHub, so future data could be easily processed and compared to the present findings. Additional work could focus on producing data analysis scripts that incorporate predictive, machine-learning algorithms to analyse the microbial communities in coral mucus or tissue and identify microbial predictors of SCTLD, similar to work that identified microbial predictors of environmental features within reef seawater microbiomes (Glasl *et al*., 2019). This could allow scientists the potential to identify corals afflicted with SCTLD before entire colonies are killed, and within the timeline of fieldwork or research cruises. Additionally, as more is learned about the identity of individual marine pathogens, then targeted pathogen identification approaches in novel systems may become more straightforward.

Conclusion

Stony Coral Tissue Loss Disease has collectively affected hundreds of kilometres of coastal and offshore reefs in the Caribbean, with no present indication of stopping. This study developed and implemented a field-based, rapid microbiome characterization pipeline in the USVI, an area more recently affected by the SCTLD outbreak. Following successful sequencing on the Illumina iSeq 100, we identified 25 SCTLD bioindicator ASVs that may represent putative pathogens, including, *V. harveyi*, a bacterium known to be pathogenic in other marine systems. Many of the 25 bioindicator ASV sequences enriched in diseased coral were recovered in near-coral seawater, a potential reservoir for pathogens and the hypothesized vector for SCTLD. Interestingly, four of the SCTLD bioindicator ASVs identified in our study exactly matched sequences previously reported as enriched in SCTLD lesion samples. Phylogenetic analysis revealed that many of the disease bioindicator ASVs were related to likely novel coral or coral-associated disease bacteria. Future investigations aimed at isolating and characterizing those microorganisms and other SCTLD bioindicator bacteria would better determine if these organisms are pathogens or opportunists, and how they potentially target and grow around or within coral hosts. In the present study, the successful integration of a rapid pipeline for studying coral disease generated data more quickly, and subsequent analysis revealed differences in microbiome structure associated with the SCTLD outbreak in the USVI. This contributes to the growing body of literature on SCTLD that is largely focused in Florida, USA. Finally, we found that this rapid microbiome characterization approach worked well for identifying microbial

bioindicators of coral disease, and it may have useful applications to marine diseases more broadly.

Experimental procedures

Sample collection

Coral colonies showing active Stony Coral Tissue Loss Disease (SCTLD) and nearby completely healthy colonies were sampled on February 11 and 13, 2020 on Buck Island (18.27883°, −64.89833°), and Black Point (18.3445°, −64.98595°) reefs, respectively, in St. Thomas, USVI (Fig. 1, Table 1). Buck Island was considered a recent outbreak site where disease first emerged in January 2020, whereas Black Point had SCTLD since at least January 2019. Coral species sampled were *M. cavernosa* (Buck Island and Black Point; SW $n = 20$, Coral, $n = 18$), *C. natans* (Buck Island and Black Point, $n = 16$), *M. meandrites* (Buck Island, $n = 9$), and *Orbicella franksi* (Buck Island, $n = 6$) (Table 1). SCTLD was identified by single or multi-focal lesions of bleached or necrotic tissue with epiphytic algae colonizing the recently dead and exposed skeleton (Fig. 2). At both reefs, some paling of colonies was apparent, especially on *Orbicella* spp., as a result of a recent bleaching event in October 2019. Due to this, it was challenging to distinguish SCTLD from white plague-type diseases, which generally occur following bleaching events (Miller *et al*., 2009). As a result, we avoided sampling *Orbicella* spp., except when it was clear the colony had regained full coloration and the disease lesion was consistent with SCTLD infection.

To investigate if putative pathogens were recoverable from seawater surrounding diseased colonies, near-coral seawater was sampled 2–5 cm away from each coral colony prior to tissue sampling via negative pressure with a 60 ml Luer-lock syringe (BD, Franklin Lakes, NJ, USA). Two seawater samples were collected over each colony displaying SCTLD lesions: one sample was taken directly above healthy tissue approximately 10 cm away from the lesion, when possible, and a second sample over diseased tissue. Syringes were placed in a dive collection bag for the duration of the dive. Once on board the boat, the seawater was filtered through a 0.22 μm filter (25 mm, Supor, Pall, Port Washington, NY, USA) and the filter with holder was placed in a Whirl-pak bag and kept on ice until returning to the shore. While on shore, filters were placed in sterile 2 ml cryovials (Simport, Beloeil, QC, Canada) and frozen in a liquid nitrogen dry shipper.

After near-coral seawater sampling, samples of tissue and mucus mixed together (referred to as coral samples) were collected. One sample was collected from each healthy colony and two from each diseased colony. For the two samples collected from each diseased colony, one was collected from the interface between healthy and newly bleached tissue (Fig. 2), and the other from healthy tissue approximately 10 cm away from the disease interface. When limited healthy tissue remained on a diseased colony, the coral sample was collected approximately 3 to 5 cm away from the disease lesion interface. The coral samples were collected with 10 ml non-Luer lock syringes (BD) by agitating and disrupting a small area of the tissue surface with the syringe tip while simultaneously aspirating the resulting suspended tissue and mucus into the syringe. To control for the significant amount of seawater and seawater-associated microbiota unavoidably captured during the collection of the coral samples, a total of nine 10 ml syringes of ambient reef seawater were collected from approximately 1 m off the reef benthos, (hereafter referred to as 'Syringe Method Control' samples). Immediately after collection, the syringes were placed in a Whirl-pak bag to prevent the loss of sample while underwater. Once back on board the boat, samples were transferred to 15 ml sterile conical tubes and placed in a 4°C cooler. Upon returning to the laboratory, samples were frozen to −20°C until analysis.

The physical and chemical environment of the surrounding seawater was characterized by measuring temperature, salinity, dissolved oxygen, pH, and turbidity using an Exo2 multiparameter sonde (YSI, Yellow Springs, OH, USA) (Supporting Information Table S1). The sonde probes were calibrated following manufacturer's protocols on the day before sampling (February 10, 2020).

DNA extraction, PCR and sequencing

Protocols for preparing samples for sequencing were specifically designed for the Illumina iSeq 100 System (Illumina Inc., San Diego, CA, USA), a portable, high-quality sequencing technology. In an approximately 1 cu. ft. size, the Illumina iSeq 100 System produces 4 million paired-end 150 bp sequence reads of high quality (<1% error rate) that can be offloaded and processed on a standard laptop without the need for Wi-Fi, making it an attractive technology to adapt for field-based microbiome studies. We brought the iSeq 100 System to a home rental in the USVI, which we transformed into a remote laboratory where we successfully conducted all DNA extractions, Polymerase Chain Reaction (PCR) and subsequent sequencing.

DNA was extracted from seawater, coral, and syringe method control samples, along with associated extraction controls, using the DNeasy PowerBiofilm Kit (Qiagen, Germantown, MD, USA). Modifications at the beginning of the extraction protocol were applied based on the sample type. For filtered seawater samples, the 0.22 μm filter was placed directly into the bead tube, and then manufacturer instructions were followed. For coral and syringe

method control samples, samples were thawed at room temperature, then immediately transferred to 4°C prior to extraction. Samples then were vortexed for 10 s and 1.8 ml of each sample was transferred to a bead tube. Samples were centrifuged at 12,045 rcf (maximum rcf available on centrifuge) for 10 min to concentrate tissue, mucus, and the associated microorganisms at the bottom of the tube, and supernatant was removed. For samples that were very clear (very little tissue collected via syringe) and for syringe method control samples, a second aliquot of 1.8 ml of sample was centrifuged on top of the existing pellet to capture more microorganisms. The extraction proceeded by following the manufacturer's protocol. Six DNA extraction controls, three for each sample type, were generated by following the manufacturer's protocol using: blank bead tubes for coral and syringe method control samples (named D1–D3) and unused 0.22 μm filters placed in bead tubes for seawater samples (named D4–D6).

A two-stage PCR process was used to prepare the samples for sequencing. In the first stage, PCR was used to amplify the V4 region of the small sub-unit ribosomal RNA (SSU rRNA) gene of bacteria and archaea. The amount of DNA added and the total reaction volume of this first PCR varied by sample type. For each PCR, 2 μl of coral and syringe method control template DNA was added to a final volume of 50 μl. 1 μl template in a 25 μl total reaction volume was used for seawater samples. For negative PCR controls, 1 or 2 μl of sterile PCR-grade water was used in 25 or 50 μl (total volume) reactions respectively. One Human Microbiome Project mock community, Genomic DNA from Microbial Mock Community B (even, low concentration), v5.1L, for 16S rRNA Gene Sequencing, HM-782D was included as a sequencing control using 1 μl DNA in a 25 μl reaction. 50 μl reactions contained 0.5 μl polymerase (GoTaq, Promega, Madison, WI, USA), 1 μl each of 10 μM forward and reverse primers, 1 μl of 10 mM dNTPs (Promega), 5 μl $MgCl_2$ (GoTaq), 10 μl 5× colourless flexi buffer (GoTaq), and 29.5 μl UV-sterilized, PCR-grade water. 25 μl reactions used the same proportions of reagents as 50 μl reactions. Earth microbiome project primers revised for marine microbiomes, 515F and 806R, targeted bacteria and archaea and were used with Illumina-specific adapters (Apprill *et al*., 2015; Parada *et al*., 2016). Two small, portable thermocyclers were used for the PCRs: the mini8 (miniPCR, Cambridge, MA, USA), which contained 8 wells and connected to a laptop for programming and initiation of the run, and the BentoLab (Bento Bioworks, London, UK), which contained 32 wells and was programmable as a unit. Using both machines was ideal because our targeted number of samples per iSeq 100 sequencing run was 40. The thermocycler programme for the first stage PCR was: 2 min at 95°C, 35 cycles (coral and syringe method control) or 28 cycles (seawater) of 20 s at 95°C, 20 s at 55°C, and 5 min at 72°C, followed by 10 min at 72°C and a final hold at 12°C. The final hold at 12°C was used due to the limitations of the BentoLab termocycler; samples were removed within an hour of the completed PCR programme and stored at 4°C until purification. The resulting PCR products from coral and syringe method control samples were purified as follows: 30 μl of PCR product per sample was mixed with 6 μl 5× loading dye (Bioline, London, UK) and separated using a 1.5% agarose gel stained with SYBR Safe DNA gel stain (Invitrogen, Thermo Fisher Scientific, Waltham, MA, USA). Bands of approximately 350 bp were excised by comparing to a 50 bp ladder (Bioline), and subsequently purified using the MinElute Gel Extraction Kit (Qiagen) following manufacturer protocols. For seawater PCR products, 5 μl of product mixed with 1 μl 5× loading dye was visualized on a 1% agarose gel to verify successful amplification, and the remaining PCR product was purified with the MinElute PCR Purification Kit (Qiagen).

The second stage PCR procedure attached unique index primers to each sample using the Nextera XT v2 set A kit (Illumina). Purified DNA (5 μl) from stage one PCR products was added to a 50 μl reaction with the following: 5 μl Nextera index primer 1, 5 μl Nextera index primer 2, 5 μl $MgCl_2$ (GoTaq), 10 μl 5× colourless buffer (GoTaq), 0.5 μl Taq polymerase (GoTaq), 1 μl of 10 mM dNTPs (Promega), and 18.5 μl UV-sterilized, PCR-grade water. The PCR was run on the BentoLab or mini8 thermocyclers with the following programme: 3 min at 95°C, 8 cycles of 30 s at 95°C, 30 s at 55°C, 30 s at 72°C, followed by 5 min at 72°C and a final hold at 12°C. A subset of PCR products were visualized on a 1% agarose gel stained with SYBR Safe DNA gel stain (Invitrogen) using 5 μl product with 1 μl 5× loading dye (BioLine) to verify bands of approximately 450 bp, indicating successful attachment of sample-specific indexes. The stage two PCR products were purified with the MinElute PCR purification kit (Qiagen) following manufacturer protocols. Purified products were quantified using the Qubit 2.0 fluorometer double-stranded DNA high sensitivity (HS) assay (Invitrogen) following manufacturer protocols to obtain stock concentrations in ng μl^{-1}. Concentrations were then converted to nM assuming average amplicon length of 450 bp and average nucleotide mass of 660 g mol^{-1}. Samples were diluted to 5 nM and pooled. Pooled samples were quantified via Qubit HS assay as before, and diluted to 1 nM, quantified again, and diluted to a loading concentration of 90 pM. A 10% spike-in of 90 pM PhiX Control v3 (Illumina) was added to the pooled 90 pM library and 20 μl of the resulting library was run on the iSeq 100 System using paired-end

150 bp sequencing with adapter removal. Samples were sequenced over three sequencing runs.

Data analysis

All R scripts used for generating ASVs and producing figures were uploaded to GitHub. Forward reads were exclusively used for the downstream processing and data analysis due to minimal overlap between forward and reverse reads. The DADA2 pipeline (v.1.17.3; with parameters: *filterAndTrim* function: trimLeft = 19, truncLen = 145, maxN = 0, maxEE = 1, rm.phix = TRUE, compress = TRUE, multithread = TRUE) was used to remove the 515F and 806R primers from all sequence reads, filter the reads for quality and chimeras, and generate amplicon sequence variants (ASVs) for each sample (Callahan *et al*., 2016). This resulted in 17,190 ASVs of the same length (126 bp) across all samples. Taxonomy was assigned using the SILVA SSU rRNA database down to the species level where applicable (v.132) (Quast *et al*., 2012). ASVs that classified to mitochondria, chloroplast, eukaryote, or an unknown Kingdom were removed from the analysis, resulting in 7366 remaining ASVs. We further filtered our dataset to remove possible contaminants introduced by DNA extraction reagents and introduced by seawater into coral samples. The R package *decontam* (v. 1.6.0) was used to identify and remove DNA extraction contaminants in all samples (seawater, coral, and syringe method control) by using a combined frequency and prevalence method employing default parameters (Davis *et al*., 2018). The method identified 26 ASV contaminants, of which only 11 contained enriched frequency in DNA extraction controls so those 11 ASVs were removed (DNA extraction contaminants summarized in Appendix 1). Because the syringe method by nature collects a significant portion of seawater, the coral samples were, in essence, 'contaminated' by seawater and thus, the microorganisms most likely derived from seawater rather than coral tissue were removed. To do this, the coral samples were compared with the nine syringe method controls (seawater collected approximately a metre off of the benthos) using the prevalence model in *decontam*, which compares the presence/absence of ASVs within the syringe method controls to the coral samples. After applying the prevalence method, analysis of the distribution of the decontam score, *P*, was conducted to determine an appropriate threshold for identifying whether an ASV was a 'contaminant' (i.e. seawater-derived) or an ASV that was tissue-associated. A threshold of 0.1 was chosen in order to be most conservative. While this conservative approach did not remove all ASVs typical of oligotrophic seawater taxa (e.g. *Synechococcus*, *Prochlorococcus*), a conservative approach here was necessary given the study goals of identifying potential SCTLD-associated ASVs residing in the surrounding seawater. The 184 ASVs identified as most prevalent in the nine syringe method controls (typically oligotrophic bacteria such as SAR11, *Prochlorococcus*, OM60 clade, *Synechococcus*, '*Candidatus* Actinomarina', AEGEAN-169 clade, etc.) were generally found at low relative abundance in the coral samples (max relative abundance = 0.0074%) and were removed from the coral sample ASV table (contaminants summarized in Appendix 2). After the ASVs identified as contaminants were removed, the coral samples and the near-coral seawater samples were re-merged into one large dataset. The re-merged dataset then was filtered to remove sparse ASVs (present at a count of 0 in the majority of samples) by removing ASVs with a count less than 0.5 when averaged across all samples. This left 2010 ASVs, which were used for all downstream analyses.

Count data were transformed to relative abundance and coral microbial communities were visualized using stacked bar charts. Data were then further log transformed following the addition of a pseudo count of one in preparation for beta diversity analyses. Bray–Curtis dissimilarity between samples was calculated using the R package *vegan* (v.2.5.7) and the resulting dissimilarities were presented in a Principal Coordinates Analysis (PCoA) (Oksanen *et al*., 2019). Permutational Analysis of Variance (PERMANOVA) with 999 permutations, using the *adonis* function in *vegan* (Oksanen *et al*., 2019), compared the Bray–Curtis dissimilarity of healthy and diseased corals to test the hypothesis that coral microbiomes are significantly different between healthy and SCTLD-afflicted samples. PERMANOVA was also used to test the hypotheses that species, reef location, and health state nested within species significantly structure the coral microbial community. We tested the same hypotheses on the near-coral seawater directly overlying the coral colony to determine if species, reef location, or health drove microbiome community structure in near-coral seawater. Dispersion of beta diversity within coral samples was calculated by measuring the distance to centroid within the PCoA as grouped by health state (HH and HD compared to DD) by implementing the *betadisper* function in *vegan* (Oksanen *et al*., 2019). Significant differences in dispersion by health state was determined by an independent Mann–Whitney *U* test. Additionally, variability of beta diversity was measured by extracting the Bray–Curtis dissimilarity values calculated within a coral condition (diseased or healthy).

To detect ASVs enriched in diseased coral compared to healthy coral, we employed the R package, *corncob* (v.0.1.0) (Martin *et al*., 2020). ASV raw counts for each sample were input into the corncob model, which models the relative abundances for each ASV with a logit-link for

mean and dispersion. Differential abundance of each ASV was modelled as a linear function of health state. Health state was defined as either healthy (healthy tissue from either apparently healthy or diseased coral) or diseased (lesion from diseased coral). The hypotheses that the relative abundance of a given ASV changed significantly with respect to coral health state were tested with the parametric Wald test. The multiple comparisons were accounted for by using a Benjamini–Hochberg false discovery rate correction with a cutoff of 0.5. Each test was conducted on the set of coral samples from an individual coral, then results were compared across corals. Following analysis of significantly differentially abundant ASVs in corals, we hypothesized that disease-associated ASVs would be recoverable in the near-coral seawater and graphed relative abundances of each disease-associated ASV in the near-coral seawater. We then employed corncob to test each identified disease-associated ASV using the differential abundance method described above to see if it was enriched at significantly higher abundances in seawater over diseased coral compared to healthy coral or apparently healthy colonies. Disease-associated ASVs were considered SCTLD bioindicators if they were enriched in diseased coral. Further, we searched for exact sequence matches between the 126 bp sequences of disease-associated ASVs reported here to the same sequence region from existing SCTLD-associated ASVs of longer lengths (approx. 253 bp) reported in other studies that also used the DADA2 pipeline. This pipeline allowed for sequences to be reported along with each ASV, enabling cross-study comparison (Callahan *et al*., 2017).

Sequences of SCTLD bioindicator ASVs, were identified to the species level, when possible, as part of the DADA2 pipeline. To obtain better genus and species-level identification of SCTLD bioindicator ASVs and to relate these ASVs to other studies of coral disease-associated bacteria, we constructed phylogenetic trees for disease-associated ASVs classifying to *Vibrio*, *Arcobacter*, Rhizobiaceae, and Rhodobacteraceae. *Vibrio* and *Arcobacter* were targeted due to their increased representation in SCTLD-associated ASVs in this study and their previous association with SCTLD (Meyer *et al*., 2019; sequences obtained from Table 1) and coral disease in general (Ben-Haim *et al*., 2003; Ushijima *et al*., 2012). Rhizobiaceae and Rhodobacteraceae were targeted for phylogenetic tree analysis given their previous association with SCTLD (Rosales *et al*., 2020; sequences obtained from Supporting Information Table S1). Phylogenetic trees of coral-associated *Vibrio* and Rhodobacteraceae bacteria previously constructed from the Coral Microbiome Database (Huggett and Apprill, 2019) were used as reference trees for the insertion of SCTLD-associated ASVs that classified as *Vibrio* or Rhodobacteraceae. Insertion of our short SCTLD-associated sequence reads was achieved using the 'quick add marked' tool in ARB (version 6.0.6.rev15220) (Ludwig, 2004). Trees produced from ARB were exported using xFig. Phylogenetic trees for *Arcobacter* and Rhizobiaceae were constructed de novo using tools from the CIPRES Science Gateway (Miller *et al*., 2010). For each tree, long-read (~1200 bp) 16S rRNA gene sequences from closely-related (>90% sequence similarity) culture collection type strains, strains isolated from the marine environment, or clone sequences from corals were recovered via BLAST searches of SCTLD-associated ASVs from the present study or previous studies (Meyer *et al*., 2019; Rosales *et al*., 2020) to the non-redundant nucleotide collection, compiled into a FASTA file, and used for a sequence alignment in MAFFT (v7.402) (Katoh, 2002). This sequence alignment was then used to generate a reference tree using RAxML-HPC (v.8) (Stamatakis, 2014) with the following commands to produce a bootstrapped maximum-likelihood best tree: raxmlHPC-HYBRID -T 4 -f a -N autoMRE -n [output_name] -s [input_alignment] -m GTRGAMMA -p 12345 -x 12345. Next, SCTLD-associated short sequence reads were compiled into a FASTA file and added to the long-read sequence alignment in MAFFT using the '--addfragments' parameter. The sequence alignment with both short and long reads and the reference tree were then used as inputs for the Evolutionary Placement Algorithm, implemented in RAxML (Berger *et al*., 2011). RAxML was called as: raxmlHPC-PTHREADS -T 12 -f v -n [output_name] -s [long_and_short_read_alignment] -m GTRGAMMA -p 12345 -t [reference_tree]. The output tree including short read sequences (RAxML_labelledTree.[output_name]) was visualized and saved using the interactive tree of life (iTOL v5.6.3) (Letunic and Bork, 2016).

Acknowledgements

The authors would like to thank Lei Ma, Joseph Townsend, Kathryn Cobleigh, Sonora Meiling, and Kelsey Beavers for field assistance and Illumina for technical assistance. Additionally, we would like to thank Laura Weber for assistance with iSeq protocol development and field assistance. This work was funded by The Tiffany & Co. Foundation, NSF EEID-2109622, OCE-1928753, OCE-1928761 and OCE-1938147, the Rockefeller Philanthropy Advisors, Dalio Foundation, and other generous donors of the Oceans 5 project. Samples were collected under permit DFW19057U. We would also like to thank Stefan Sievert, Harriet Alexander, and Tami Lieberman for helpful comments on the manuscript.

References

Aeby, G.S., Ushijima, B., Campbell, J.E., Jones, S., Williams, G.J., Meyer, J.L., *et al*. (2019) Pathogenesis of a

tissue loss disease affecting multiple species of corals along the Florida Reef Tract. *Front Mar Sci* **6**: 678.

Apprill, A. (2019) On-site sequencing speeds up and redirects field-based microbiology. *Env Microbiol Rep* **11**: 45–47.

Apprill, A., McNally, S., Parsons, R., and Weber, L. (2015) Minor revision to V4 region SSU rRNA 806R gene primer greatly increases detection of SAR11 bacterioplankton. *Aquat Microb Ecol* **75**: 129–137.

Ben-Haim, Y., Thompson, F.L., Thompson, C.C., Cnockaert, M.C., Hoste, B., Swings, J., and Rosenberg, E. (2003) *Vibrio coralliilyticus* sp. nov., a temperature-dependent pathogen of the coral *Pocillopora damicornis*. *Int J Syst Evol Micr* **53**: 309–315.

Berger, S.A., Krompass, D., and Stamatakis, A. (2011) Performance, accuracy, and web server for evolutionary placement of short sequence reads under maximum likelihood. *Syst Biol* **60**: 291–302.

Burge, C.A., Kim, C.J.S., Lyles, J.M., and Harvell, C.D. (2013) Special issue oceans and humans health: the ecology of marine opportunists. *Microb Ecol* **65**: 869–879.

Callahan, B.J., McMurdie, P.J., and Holmes, S.P. (2017) Exact sequence variants should replace operational taxonomic units in marker-gene data analysis. *ISME J* **11**: 2639–2643.

Callahan, B.J., McMurdie, P.J., Rosen, M.J., Han, A.W., Johnson, A.J.A., and Holmes, S.P. (2016) DADA2: high-resolution sample inference from Illumina amplicon data. *Nat Methods* **13**: 581–583.

Chen, Y.-H., Yang, S.-H., Tandon, K., Lu, C.-Y., Chen, H.-J., Shih, C.-J., and Tang, S.-L. (2021) Potential syntrophic relationship between coral-associated *Prosthecochloris* and its companion sulfate-reducing bacterium unveiled by genomic analysis. *Microb*, **7**: 1–14.

Davis, N.M., Proctor, D.M., Holmes, S.P., Relman, D.A., and Callahan, B.J. (2018) Simple statistical identification and removal of contaminant sequences in marker-gene and metagenomics data. *Microbiome* **6**: 226.

Dobbelaere, T., Muller, E.M., Gramer, L.J., Holstein, D.M., and Hanert, E. (2020) Coupled epidemio-hydrodynamic modeling to understand the spread of a deadly coral disease in Florida. *Front Mar Sci* **7**: 591881.

Egan, S., and Gardiner, M. (2016) Microbial dysbiosis: rethinking disease in marine ecosystems. *Front Microbiol* **7**: 991.

Florida Keys National Marine Sanctuary (2018) Case Definition: Stony Coral Tissue Loss Disease (SCTLD).

Glasl, B., Bourne, D.G., Frade, P.R., Thomas, T., Schaffelke, B., and Webster, N.S. (2019) Microbial indicators of environmental perturbations in coral reef ecosystems. *Microbiome* **7**: 94.

Grimes, D.J., Stemmler, J., Hada, H., May, E.B., Maneval, D., Hetrick, F.M., *et al*. (1984) *Vibrio* species associated with mortality of sharks held in captivity. *Microb Ecol* **10**: 271–282.

Huggett, M.J., and Apprill, A. (2019) Coral microbiome database: integration of sequences reveals high diversity and relatedness of coral-associated microbes. *Env Microbiol Rep* **11**: 372–385.

Illumina. (2020) *iSeq 100 Sequencing System Specification Sheet*. San Diego, California, United States: Illumina.

Katoh, K. (2002) MAFFT: a novel method for rapid multiple sequence alignment based on fast Fourier transform. *Nucleic Acids Res* **30**: 3059–3066.

Kramer, P.R., Roth, L., and Lang, J. (2021) *Map of Stony Coral Tissue Loss Disease Outbreak in the Caribbean*.

Letunic, I., and Bork, P. (2016) Interactive tree of life (iTOL) v3: an online tool for the display and annotation of phylogenetic and other trees. *Nucleic Acids Res* **44**: W242–W245.

Liu, M., Huang, Z., Zhao, Q., and Shao, Z. (2019) *Cohaesibacter intestini* sp. nov., isolated from the intestine of abalone, *Haliotis discus hannai*. *Int J Syst Evol Microbiol* **69**: 3202–3206.

Liu, P.-Y., Wu, W.-K., Chen, C.-C., Panyod, S., Sheen, L.-Y., and Wu, M.-S. (2020) Evaluation of compatibility of 16S rRNA V3V4 and V4 amplicon libraries for clinical microbiome profiling. *Microbiology*. https://doi.org/10.1101/2020.08.18.256818

Ludwig, W. (2004) ARB: a software environment for sequence data. *Nucleic Acids Res* **32**: 1363–1371.

Luna, G.M., Bongiorni, L., Gili, C., Biavasco, F., and Danovaro, R. (2010) *Vibrio harveyi* as a causative agent of the white syndrome in tropical stony corals. *Env Microbiol Rep* **2**: 120–127.

MacKnight, N.J., Cobleigh, K., Lasseigne, D., Chaves-Fonnegra, A., Gutting, A., Dimos, B., *et al*. (2021) Microbial dysbiosis reflects disease resistance in diverse coral species. *Commun Biol* **4**: 679.

Martin, B.D., Witten, D., and Willis, A.D. (2020) Modeling microbial abundances and dysbiosis with beta-binomial regression. *Ann Appl Stat* **14**: 94–115.

Meiling, S., Muller, E.M., Smith, T.B., and Brandt, M.E. (2020) 3D photogrammetry reveals dynamics of stony coral tissue loss disease (SCTLD) lesion progression across a thermal stress event. *Front Mar Sci* **7**: 597643.

Mera, H., and Bourne, D.G. (2018) Disentangling causation: complex roles of coral-associated microorganisms in disease: disentangling coral disease causation. *Environ Microbiol* **20**: 431–449.

Meyer, J.L., Castellanos-Gell, J., Aeby, G.S., Häse, C.C., Ushijima, B., and Paul, V.J. (2019) Microbial community shifts associated with the ongoing stony coral tissue loss disease outbreak on the Florida Reef Tract. *Front Microbiol* **10**: 2244.

Miller, J., Muller, E., Rogers, C., Waara, R., Atkinson, A., Whelan, K.R.T., *et al*. (2009) Coral disease following massive bleaching in 2005 causes 60% decline in coral cover on reefs in the US Virgin Islands. *Coral Reefs* **28**: 925–937.

Miller, M.A., Pfeiffer, W., and Schwartz, T. (2010) Creating the cipres science gateway for inference of large phylogenetic trees, pp. 1–8.

Muller, E.M., Sartor, C., Alcaraz, N.I., and van Woesik, R. (2020) Spatial epidemiology of the stony-coral-tissue-loss disease in Florida. *Front Mar Sci* **7**: 163.

Neely, K.L., Macaulay, K.A., Hower, E.K., and Dobler, M.A. (2020) Effectiveness of topical antibiotics in treating corals affected by Stony Coral Tissue Loss Disease. *PeerJ* **8**: e9289.

Oksanen, J., Blanchet, F.G., Friendly, M., Kindt, R., Legendre, P., McGlinn, D., et al. (2019) vegan: community ecology package. *R package version 25-4*.

Parada, A.E., Needham, D.M., and Fuhrman, J.A. (2016) Every base matters: assessing small subunit rRNA primers for marine microbiomes with mock communities, time series and global field samples. *Environ Microbiol* **18**: 1403–1414.

Pedersen, K., Verdonck, L., Austin, B., Austin, D.A., Blanch, A.R., Grimont, P.A.D., *et al*. (1998) Taxonomic evidence that *Vibrio carchariae* Grimes et al, 1985 is a junior synonym of *Vibrio harveyi* (Johnson and Shunk 1936) Baumann et al. 1981. *Int J Syst Bacteriol* **48**: 749–758.

Precht, W.F., Gintert, B.E., Robbart, M.L., Fura, R., and van Woesik, R. (2016) Unprecedented disease-related coral mortality in southeastern Florida. *Sci Rep* **6**: 31374.

Qu, L., Lai, Q., Zhu, F., Hong, X., Sun, X., and Shao, Z. (2011) *Cohaesibacter marisflavi* sp. nov., isolated from sediment of a seawater pond used for sea cucumber culture, and emended description of the genus *Cohaesibacter*. *Int J Syst Evol Microbiol* **61**: 762–766.

Quast, C., Pruesse, E., Yilmaz, P., Gerken, J., Schweer, T., Yarza, P., *et al*. (2012) The SILVA ribosomal RNA gene database project: improved data processing and web-based tools. *Nucleic Acids Res* **41**: D590–D596.

Rosales, S.M., Clark, A.S., Huebner, L.K., Ruzicka, R.R., and Muller, E.M. (2020) *Rhodobacterales* and *Rhizobiales* are associated with stony coral tissue loss disease and its suspected sources of transmission. *Front Microbiol* **11**: 681.

Silveira, C.B., Gregoracci, G.B., Coutinho, F.H., Silva, G.G. Z., Haggerty, J.M., de Oliveira, L.S., *et al*. (2017) Bacterial community associated with the reef coral *Mussismilia braziliensis's* momentum boundary layer over a diel cycle. *Front Microbiol* **8**: 784.

Soffer, N., Brandt, M.E., Correa, A.M., Smith, T.B., and Thurber, R.V. (2014) Potential role of viruses in white plague coral disease. *ISME J* **8**: 271–283.

Stackebrandt, E., and Goebel, B.M. (1994) Taxonomic note: a place for DNA–DNA reassociation and 16S rRNA sequence analysis in the present species definition in bacteriology. *Int J Syst Evol Microbiol* **44**: 846–849.

Stamatakis, A. (2014) RAxML version 8: a tool for phylogenetic analysis and post-analysis of large phylogenies. *Bioinformatics* **30**: 1312–1313.

Ushijima, B., Smith, A., Aeby, G.S., and Callahan, S.M. (2012) *Vibrio owensii* induces the tissue loss disease *Montipora* white syndrome in the Hawaiian reef coral *Montipora capitata*. *PLoS ONE* **7**: e46717.

Vega Thurber, R., Mydlarz, L.D., Brandt, M., Harvell, D., Weil, E., Raymundo, L., *et al*. (2020) Deciphering coral disease dynamics: integrating host, microbiome, and the changing environment. *Front Ecol Evol* **8**: 575927.

VI-CDAC (2021) Virgin Islands Coral Disease. *Stony Coral Tissue Loss Disease in the US Virgin Islands*.

Viehman, S., Mills, D., Meichel, G., and Richardson, L. (2006) Culture and identification of *Desulfovibrio* spp. from corals infected by black band disease on Dominican and Florida keys reefs. *Dis Aquat Organ* **69**: 119–127.

Walton, C.J., Hayes, N.K., and Gilliam, D.S. (2018) Impacts of a regional, multi-year, multi-species coral disease outbreak in southeast Florida. *Front Mar Sci* **5**: 323.

Wang, Q., Garrity, G.M., Tiedje, J.M., and Cole, J.R. (2007) Naïve Bayesian classifier for rapid assignment of rRNA sequences into the new bacterial taxonomy. *AEM* **73**: 5261–5267.

Weber, L., Gonzalez-Díaz, P., Armenteros, M., and Apprill, A. (2019) The coral ecosphere: a unique coral reef habitat that fosters coral–microbial interactions. *Limnol Oceanogr* **9999**: 1–16.

Supporting Information

Additional Supporting Information may be found in the online version of this article at the publisher's web-site:

Appendix S1: Supporting information.

Appendix S2: Supporting information.

Appendix S3: Supporting information.